Research article

Identification of ALDOB as a novel prognostic biomarker in kidney clear cell renal cell carcinoma

Xiao-yang Li [a],[1], You-yao Xu [a],[*],[1], Sen-yan Wu [a], Xi-xi Zeng [a],[b], Yan Zhou [a],[c], Guo-bin Cheng [a],[**]

[a] The Quzhou Affiliated Hospital of Wenzhou Medical University, Quzhou People's Hospital, Quzhou, China
[b] The Joint Innovation Center for Health and Medicine, Quzhou People's Hospital, The Quzhou Afliated Hospital of Wenzhou Medical University, Quzhou, China
[c] Department of Nephrology, Quzhou People's Hospital, The Quzhou Afliated Hospital of Wenzhou Medical University, Quzhou, China

ABSTRACT

Kidney clear cell renal cell carcinoma (KIRC) is also the most lethal subtype among all kidney cancer subtypes, posing a severe threat to public health. Therefore, it is crucial to identify new, reliable biomarkers in KIRC. Therefore, it is crucial to identify novel, reliable biomarkers associated with KIRC. We analyzed RNA sequence results from TCGA and several GEO datasets. The commonly deregulated gene, ALDOB, was found in multiple data and confirmed its important prognostic value. Subsequently, we explored the specific mechanism by which ALDOB regulates anti-tumor immunity through in vivo and in vitro experiments. We found that ALDOB may play a role in regulating tumor growth by regulating CD8$^+$ T cell infiltration. This is consistent with the results of our immune infiltration-related analysis. In addition, we have also discovered the effect of ALDOB in previous studies on other cancer types. Finally, we concluded that ALDOB may have potential reference value for immunotherapy and can also be used as an independent predictor of prognosis in KIRC.

1. Introduction

Renal cell carcinoma (RCC) is a commonly occurring tumor within the urinary system. Among its various subtypes, kidney clear cell renal cell carcinoma (KIRC) is the most prevalent, constituting approximately 80 %–90 % of all cases [1–3]. Unfortunately, KIRC is also the most lethal subtype among all kidney cancer subtypes [4]. Traditional treatments such as radiotherapy and chemotherapy have shown limited efficacy, making surgical resection the primary treatment option [5,6]. However, a significant number of patients experience recurrence after surgery, with around 30 % of patients developing metastasis. Early diagnosis of KIRC is crucial for patient treatment and prognosis [7]. Therefore, the identification of new and reliable biomarkers associated with KIRC is of utmost importance.

One area of interest in cancer research is the gene expression of metabolic enzymes in tumors. These enzymes play crucial roles in various cellular processes such as cell cycle regulation, DNA damage repair, cell proliferation, apoptosis, and tumor microenvironment regulation. Thus, they can influence the progression of cancer and serve as potential prognostic markers. For instance, FASN, a key enzyme in lipid metabolism, has been found to be overexpressed in colon cancer tissue compared to adjacent tissue [8]. Moreover, the

concentration of FASN in serum has been positively correlated with the clinical stage of colon cancer [9]. Additionally, mutations in metabolic enzymes can directly contribute to tumorigenesis. The IDH1/2 metabolic genes, for example, are frequently mutated in various human cancers [10,11]. These mutations disrupt cell metabolism and epigenetic regulation, thereby promoting tumorigenesis. IDH1, in particular, is an important molecular marker in patients with glioma and acute myeloid leukemia [10,12].

With advancements in molecular biology and genetic molecular biology, numerous studies have confirmed the association between the occurrence and progression of KIRC and differential gene expression [13–15]. In this study, we utilized RNA data obtained from GEO and TCGA databases to identify differentially expressed genes associated with disease progression. Various bioinformatics algorithms and software were employed to explore functional pathways related to these genes. To further validate our findings, a key candidate biomarker was identified and analyzed for its clinical significance. Finally, we investigated the molecular mechanisms by which this biomarker exerts its effects in KIRC.

By understanding the molecular mechanisms and identifying potential biomarkers associated with KIRC, we aim to contribute to the development of effective diagnostic tools, treatment strategies, and improved patient outcomes.

2. Methods

2.1. Data preprocessing

We collected gene expression data from a total of 608 KIRC patients and their corresponding clinical information from the TCGA database. Additionally, we retrieved three independent gene expression profiles along with clinical data from the GEO database. These included GSE100666, which consisted of three KIRC samples and three normal renal samples, GSE53757, which included 72 KIRC samples and 72 normal renal samples, and GSE12606, which contained three KIRC samples and three normal renal samples. To ensure the reliability of our analysis, we performed various preprocessing steps on the obtained gene expression profiles. This involved quality control measures, data filtering to eliminate any irrelevant or unreliable data, background correction, and conversion of the ensemble ID numbers to the corresponding gene names.

2.2. Differentially expressed gene identification

The expression levels of KIRC samples and normal renal samples were compared with the "limma" R package [16]. We identified the different expression genes (DEGs) with the standard: adj. P < 0.01 and |Log2FC| >2. The volcano plot depicting Differentially Expressed Genes (DEGs) and the Venn diagram illustrating their overlap were generated using the "ggplot2" and "VennDiagram" packages, respectively.

2.3. Immune infiltration analysis

We first used the Timer Web server [17] to conduct a series of analyses on the expression of ALDOB and the infiltration abundance of immune cells in KIRC through the gene module. For more detailed characterization of immune cell types, we employed the "CIBERSORT" [18] R package, which utilizes gene expression data to estimate the abundance of individual cell types within a heterogeneous cell population. This approach was utilized to investigate potential correlations between ALDOB expression and immune cell populations.

2.4. Cell lines and reagent

The KIRC cell lines 786-O and ACHN were obtained from the Shanghai Institute of Biochemistry and Cell Biology, Chinese Academy of Sciences in Shanghai, China. The 786-O cells were cultured in RPMI-1640 medium, while the ACHN cells were cultured in DMEM medium. Both media were supplemented with 10 % fetal bovine serum (FBS) and 1 % Pen/Strep. The RCC4 cells were cultured in McCOY's 5A medium supplemented with 10 % FBS and 1 % Pen/Strep. The Renca cells, on the other hand, were cultured in 1640 medium supplemented with 10 % FBS, 1 % Pen/Strep, non-essential amino acids (NEAA) at an extra concentration of 0.1 mM, sodium pyruvate at an extra concentration of 1 mM, and L-glutamine at an extra concentration of 2 mM. All cell lines were maintained in a controlled environment at 37 °C with a CO_2 concentration of 5 %. Regular assessments for mycoplasma contamination were carried out using PCR techniques.

2.5. Overexpression and depletion of genes in cell lines

Stable overexpression of ALDOB was achieved in 786-O, ACHN, RCC4, and Renca cells by infecting them with Flag-ALDOB lentiviral particles (Miaoling Biology). Cells were then incubated for 48 h and subsequently selected in a medium containing 5 μg/ml puromycin for 7 days to enhance ALDOB expression. To generate ALDOB knockdown (KD) cells, human ALDOB shRNA plasmid and mouse ALDOB shRNA plasmid (Miaoling Biology) were transfected into the aforementioned cell lines. Following transfection, cells were sorted based on green fluorescent protein (GFP) fluorescence to isolate successful ALDOB knockdown cells. Subsequently, PCR and Western blot analyses were conducted to assess the efficiency of ALDOB overexpression or depletion.

2.6. Western blot analysis

Cells were lysed in ice-cold RIPA lysis buffer containing 1 mM phenylmethanesulfonyl fluoride to extract proteins. Protein concentration in the lysates was determined using the BCA protein assay kit. Equal amounts of total protein were separated on 10 % SDS-PAGE and transferred onto a PVDF membrane. The membrane was then incubated with specific antibodies against ALDOB and β-actin. After washing with TBST, the membranes were exposed to HRP-conjugated secondary antibodies and visualized using a ChemiScopeTouch imaging system. The intensity of immunoblot bands was quantified using ImageJ 1.8.0 software.

2.7. Colony formation assay

Cells from various experimental groups were plated at a density of 5000 cells per well in 6-well plates and incubated for 10–14 days with regular medium changes every two days to support colony growth. After the incubation period, colonies were rinsed with PBS, fixed with 4 % formaldehyde for 30 min, and stained with 0.5 % crystal violet in 10 % methanol for another 30 min. Subsequently, the plates were washed, air-dried, and examined for colony visualization.

2.8. Cell growth assay

For cell growth assessment, cells from different experimental groups were seeded in 6-well plates at a density of 10000 cells per well. The cell numbers were subsequently quantified on days 2, 4, and 6 post-seeding to compare growth rates.

2.9. In vitro wound healing assay

For in vitro wound healing assays, cells were cultured in complete medium in 6-well plates until reaching approximately 100 % confluence. Subsequently, the cells were serum-deprived for 12 h at 37 °C and 5 % CO_2. A scratch was created using a 1000 μl pipette tip, followed by washing the wells with phosphate-buffered saline and replacing the medium with serum-free medium. Images were captured at 0 h and 24 h post-scratching. The width of the scratch at both time points was measured, and wound closure percentage was calculated using the formula: % wound closure = ((0 h wound area – 24 h wound area) × 100)/0 h wound area.

2.10. Transwell assay

For the cell migration assay utilizing transwell filter inserts with 8 μm pore size, 5×10^4 cells (786-O) or 2×104 cells (Renca) in serum-free medium were added to the upper chamber of each insert. The inserts were then placed in a 24-well plate containing 500 μl of complete medium. Following a 12-h incubation at 37 °C, cells in the upper chamber were gently removed, while the migrated cells were fixed with methanol and stained with 0.05 % crystal violet solution (100 μl). Subsequently, the inserts were examined under an inverted microscope (100 × magnification), and images of five fields per insert were captured. The migrated cells stained with crystal violet were quantified and compared.

2.11. Animal care and use

The animal study was approved by the Animal Ethics Committee of Quzhou People's Hospital. Male 6-week-old Balb/c mice and Nude mice were obtained from the Nanjing Biomedical Research Institute of Nanjing University. For the study, 8-week-old male BALB/c nude mice or Nude mice were subcutaneously injected with 5×105 Renca, Renca ALDOB OE, or Renca ALDOB KD cells in the right flank. The growth of the subcutaneous tumors was monitored by caliper measurements, and tumor volume was calculated using the formula: length × width [2] × 0.5. The ethical guidelines limited the tumor size to 2000 mm^3 per mouse, and this threshold was strictly adhered to throughout the study. Upon sacrifice, the tumors were excised, weighed, and preserved in 10 % formaldehyde for further analysis. Quzhou People's Hospital Ethics Committee approved this study (ID: 20220121003).

2.12. IHC staining

Immunohistochemistry (IHC) staining was performed to evaluate the expression of CD8 in formalin-fixed paraffin-embedded mouse tumor tissue sections. The slides, with a thickness of approximately 3–5 μm, underwent a heat-induced epitope retrieval process at 68 °C for 60 min. Subsequently, the slides were deparaffinized and rehydrated. Following preparation, specific primary antibodies targeting CD8 were applied and allowed to incubate overnight at 4 °C. This was followed by exposure to a biotin-conjugated secondary antibody at room temperature for 30 min. Visualization of the proteins was achieved using the Diaminobenzidine Chromogen Kit (BDB2004, Biocare). To improve visibility, the slides were counterstained with diluted hematoxylin and examined under a light microscope. Representative images were captured using ZEN Connect software from Zeiss. The IHC staining facilitated the quantification of the protein signal by utilizing Image J software.

2.13. Warburg effect assessment

In order to assess the Warburg effect, tumor cells with different gene expression profiles (WT, ALDOB overexpression, and ALDOB
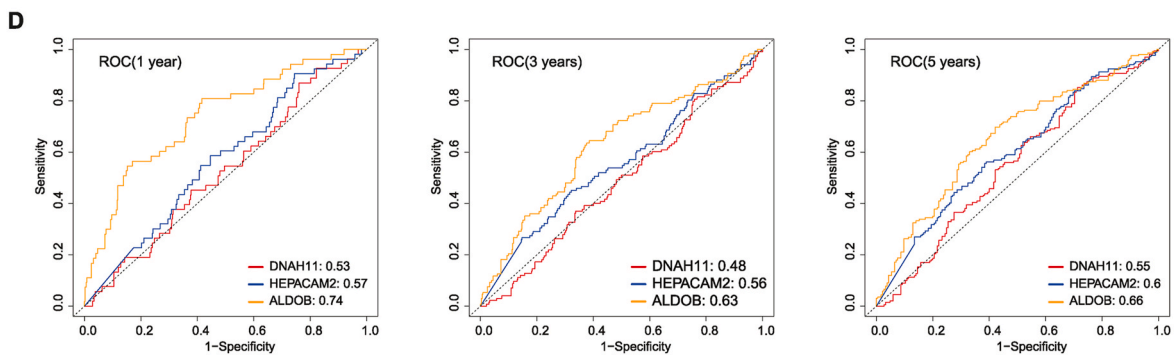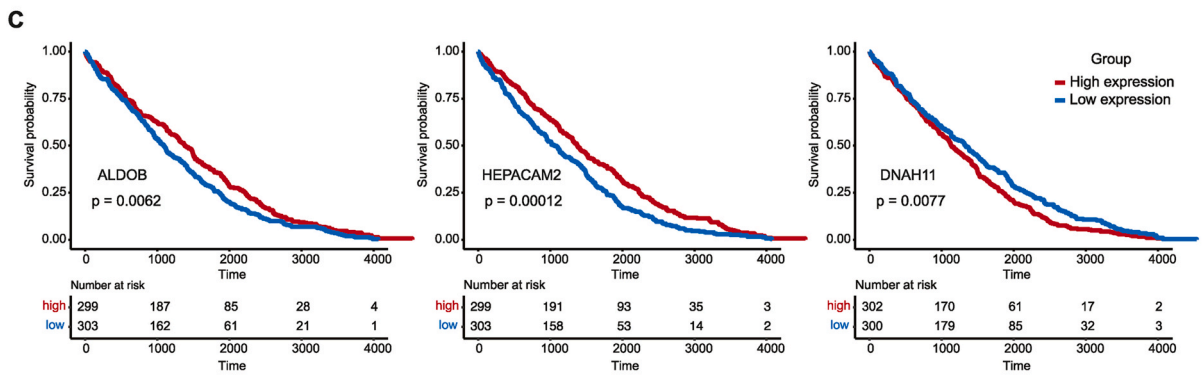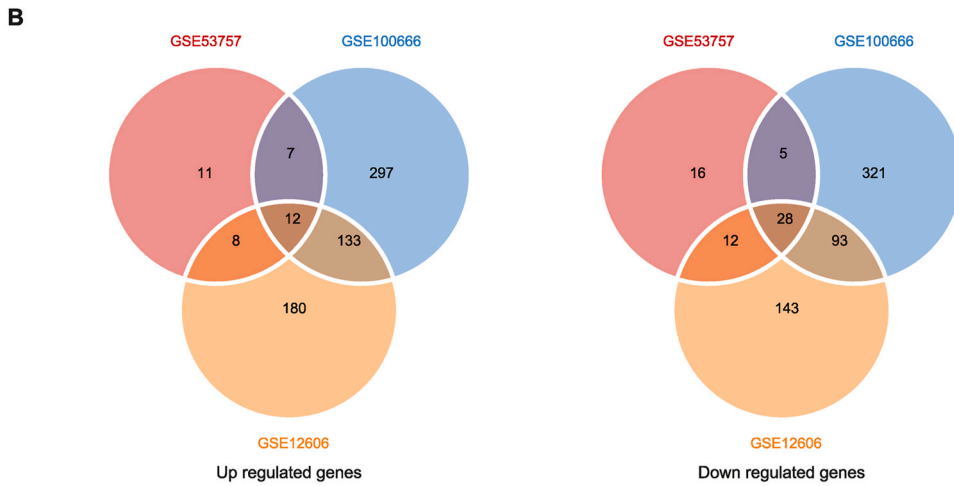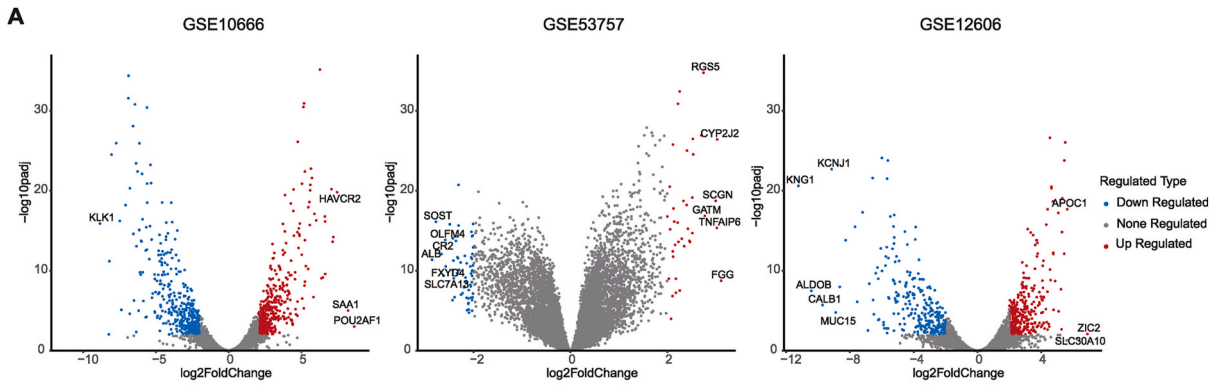
(caption on next page)

Fig. 1. Identification of the prognosis gene. **A** The volcano plots of three GSE (GSE100666, GSE53757, and GSE12606) project DEGs; **B** The Venn diagram of overlapping DEGs; **C** The Kaplan-Meier survival curve of three candidate prognosis genes (ALDOB, HEPACAM2, and DNAH11); **D** The ROC curve of three candidate prognosis genes (ALDOB, HEPACAM2, and DNAH11). Abbreviations: TCGA.

knockdown) were cultured and subjected to metabolic analysis. Colorimetric assay kits for measuring glucose consumption (Sigma, MAK083-1 KT) and lactate production (Sigma, MAK065-1 KT) were utilized following the manufacturer's instructions. The rates of glucose consumption and lactate production were determined using an iMark™ Microplate Reader (Bio-Rad, 168–1130). To account for potential variations in cell proliferation induced by growth factors, the measured values were normalized to the cell number.

2.14. Statistical analyses

Kaplan-Meier curves generated with the "survival" R package were used to display survival-related analysis results. The P value was determined by a log-rank test. The receiver operating characteristic (ROC) curve over time was used to show the accuracy of the biomarker. We did the ROC analysis with the "pROC" R package. In the other statistical analysis parts, we used unpaired two-tailed Student's t-test. And all these data analyses were performed using the R program (R 4.2.1).

3. Results

3.1. Identification of differentially expressed genes

We conducted a comparative analysis of the gene expression between KIRC samples and normal renal samples using data from three GSE (GSE100666, GSE53757, and GSE12606) projects. To identify differentially expressed genes (DEGs) in KIRC samples relative to normal tissues, we implemented stringent filtering criteria. Specifically, we required an adjusted p-value of less than 0.01 and a fold change greater than 2 ($|Log2FC| > 2$). Subsequently, we visually represented the DEGs using a volcano plot (Fig. 1A). To increase the reliability of our findings, we considered genes that displayed consistent trends across multiple projects as more likely to be associated with the occurrence and progression of the disease. By overlapping the DEGs identified in these three projects, we discovered 12 up-regulated genes and 28 down-regulated genes that were consistently dysregulated in KIRC samples compared to normal tissues (Fig. 1B). We have meticulously compiled a comprehensive list of these genes in Table 1.

3.2. Identification of the prognosis gene

To gain insights into the potential impact of these 40 genes on the development of KIRC, we performed a survival analysis using gene expression data and prognostic information obtained from the TCGA database. Using a significance threshold of $p < 0.01$, we identified three genes: ALDOB, HEPACAM2, and DNAH11, which showed significant associations with the prognosis of KIRC patients (Fig. 1C). To determine the most promising prognostic gene among these candidates, we conducted a receiver operating characteristic (ROC) analysis. Remarkably, ALDOB emerged as the gene with the most remarkable prognostic potential, as it demonstrated superior performance in the ROC analysis (TCGA, All patients: 1 year AUC = 0.74; 3 years AUC = 0.63; 5 years AUC = 0.66) (Fig. 1D). These findings provide compelling evidence that ALDOB could serve as a robust prognostic marker in KIRC.
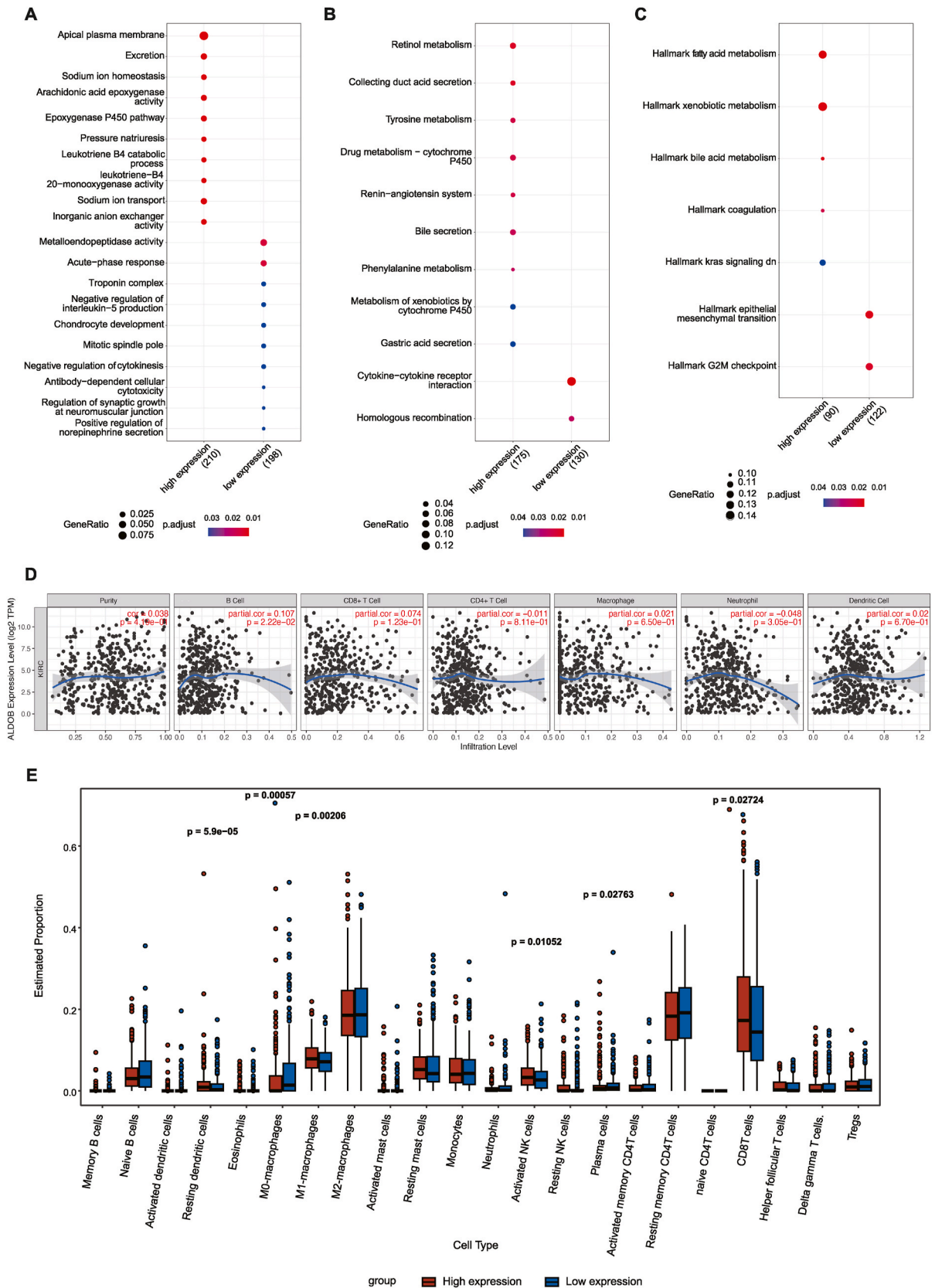
3.3. ALDOB-related pathway analysis

After identifying ALDOB as a potential prognostic biomarker for KIRC, we aimed to explore the underlying pathways through which it exerts its effects. Utilizing RNA data from 608 KIRC patients sourced from the TCGA database, we stratified them into two groups based on the median expression of ALDOB: a high-expression ALDOB group and a low-expression ALDOB group. Subsequently, we conducted differential gene expression analysis between these two groups. The differentially expressed genes were then subjected to Gene Ontology (GO) analysis, Kyoto Encyclopedia of Genes and Genomes (KEGG) analysis, and Hallmark pathway enrichment analysis to elucidate the biological processes and pathways associated with ALDOB expression in KIRC (Fig. 2A–C). In the GO pathway enrichment analysis, we observed that the high-expression ALDOB group exhibited significant associations with pathways related to excretion, pressure natriuresis, and acute-phase response (Fig. 2A). These findings suggest that patients in the high-expression ALDOB group may exhibit stronger clinical responses to treatment. Furthermore, the KEGG pathway enrichment analysis revealed that retinol metabolism, tyrosine metabolism, bile secretion, and phenylalanine metabolism were enriched in the high-expression ALDOB group, all of which are related to the upstream and downstream pathways of glycolysis (Fig. 2B). Consistently, the Hallmark pathway

Table 1
Lists 12 overlapping up-regulated genes and 28 overlapping down-regulated genes.

DEGs	Gene names
up-regulated	DNAH11, CCND1, ANGPT2, HEY1, VWF, TNFAIP6, COL23A1, SLC6A3, CA9, ANGPTL4, HILPDA, NDUFA4L2
down-regulated	SOST, C16orf89, TFAP2B, RIMBP2, ELF5, ATP6V1C2, GGACT, RHBG, TMEM52B, RHCG, FXYD4, CLCNKA, HEPACAM2, SERPINA5, ATP6V0D2, TDGF1, TMEM213, DPEP1, HRG, KCNJ1, UMOD, CTXN3, CLDN8, RALYL, CALB1, XPNPEP2, KNG1, ALDOB

(caption on next page)

Fig. 2. ALDOB-related pathway analysis and immune cell infiltration analysis in KIRC. **A** GO pathway enrichment analysis; **B** KEGG pathway enrichment analysis; **C** Hallmark pathway enrichment analysis; **D** The association between immune cells and ALDOB expression in TIMER website; **E** Relationship between ALDOB expression and immune cells in the "CIBERSORT" database.

enrichment analysis also revealed a significant association between ALDOB expression and bile acid metabolism (Fig. 2C). Collectively, these results indicate that the role of the ALDOB gene in renal cancer is closely intertwined with glycolysis. Overall, our findings suggest that ALDOB may exert its prognostic potential in KIRC through its involvement in key pathways, primarily those related to glycolysis. These insights shed light on the underlying mechanisms and lay the groundwork for further exploration of the functional role of ALDOB in KIRC.

3.4. The immune cell infiltration landscape in KIRC

To delve deeper into the relationship between ALDOB expression and the immune landscape of KIRC, we performed immune infiltration analysis using the TIMER website and the "CIBERSORT" R package (Fig. 2D and E). Fig. 2D illustrates the relationship between ALDOB expression levels and the infiltration of various immune cell types in KIRC. It is apparent from the analysis that ALDOB expression in KIRC exhibits a significant association with the infiltration of B cells ($p = 2.22e-02$), CD8$^+$ T cells ($p = 1.23e-01$), and neutrophil cells ($p = 3.05e-01$). Notably, the infiltration of B cells and CD8$^+$ T cells showed a positive correlation with ALDOB expression, whereas the infiltration of neutrophil cells displayed a negative correlation (Fig. 2D). Additionally, we utilized the "CIBERSORT" package for immune infiltration analysis, which provides a comprehensive assessment of immune cell categories using linear support vector regression for deconvolution analysis. The results revealed significant associations between ALDOB expression and the infiltration of resting dendritic cells ($p = 5.9e-05$), M0-macrophages ($p = 0.00057$), M1-macrophages ($p = 0.00206$), activated NK cells ($p = 0.01052$), plasma cells ($p = 0.02763$), and CD8$^+$ T cells ($p = 0.02724$) in KIRC (Fig. 2E). Both analysis tools consistently demonstrated a significant correlation between ALDOB expression and the infiltration of CD8$^+$ T cells in KIRC. In conclusion, our findings indicate that ALDOB expression is associated with the infiltration of various immune cell types, suggesting its potential value in immunotherapy for KIRC. The positive correlation with CD8$^+$ T cell infiltration further highlights the potential immunotherapeutic implications of ALDOB in KIRC.

3.5. ALDOB inhibits the growth and migration of RCC cells in vitro

To investigate the biological function of ALDOB in tumor progression and its association with renal cell carcinoma (RCC), we conducted ALDOB overexpression and knockdown experiments in human renal cancer cell lines (786-O, RCC4, ACHN) and a mouse renal cancer cell line (Renca). The efficacy of ALDOB overexpression and knockdown was confirmed through Western blot experiments (Supplementary Fig. 2). In colony formation assays, we observed that overexpression of ALDOB significantly suppressed the formation of tumor cell colonies, whereas ALDOB knockdown notably promoted colony formation (Fig. 3A, Supplementary Fig. 3A). These results suggest that ALDOB plays a pivotal role in regulating the clonal growth ability of renal cancer cells. In line with these findings, cell growth experiments demonstrated that ALDOB overexpression markedly suppressed the growth rate of renal cancer cell lines, whereas ALDOB knockdown conversely accelerated the growth rate of renal cancer cells (Fig. 3B, Supplementary Fig. 3B). These findings suggest that ALDOB may serve as a potential regulator of cellular proliferation in RCC. Furthermore, wound healing assays were conducted to assess the migratory ability of cells. Overexpression of ALDOB significantly inhibited the migration ability of 786-O and Renca cells, whereas ALDOB knockdown notably promoted their migration ability (Fig. 3C and D). In addition, the cell transwell assay demonstrated that ALDOB expression significantly decreased the number of migrating cells in both 786-O and Renca cells (Supplementary Fig. 4). Overall, these experimental results indicate that ALDOB exerts a significant impact on tumor cell colony formation, cell growth, and cell migration in RCC. The outcomes of ALDOB overexpression and knockdown experiments collectively support its potential role as a key factor in the regulation of RCC progression.

We further explored the impact of ALDOB on tumor cell metabolism following its implication in glycolysis based on RNA-seq analysis. Our investigation revealed that ALDOB overexpression (OE) led to a decrease in medium acidification in renal cancer cell lines, indicative of suppressed cancer cell metabolism (Supplementary Fig. 5A). Conversely, ALDOB knockdown (KD) accelerated medium acidification, suggesting enhanced cancer cell metabolism (Supplementary Fig. 5A). Furthermore, ALDOB KD promoted glucose consumption and lactate production, characteristic features of the Warburg effect, while ALDOB OE significantly inhibited these metabolic processes (Supplementary Fig. 5B).

3.6. Regulation of anti-tumor immunity by ALDOB

To further confirm the impact of ALDOB on tumor growth and its role in anti-tumor immunity, we conducted in vivo experiments by injecting ALDOB WT and ALDOB OE Renca cells into nude mice and Balb/c mice subcutaneously (Fig. 4A–D). Interestingly, we found that overexpression of ALDOB effectively inhibited the growth rate of renal cancer tumors in mice. However, this inhibitory effect was more pronounced in immune-intact Balb/c mice (Fig. 4B–C, Fig. 4E and F). Additionally, we observed an increase in infiltrated CD8$^+$ T cells in the ALDOB OE Renca group (Supplementary Fig. 6A). These findings suggest that ALDOB overexpression may activate anti-tumor immunity within the tumors, contributing to the suppression of tumor growth. Furthermore, we performed similar experiments by injecting ALDOB WT and ALDOB KD Renca cells into nude mice and Balb/c mice subcutaneously (Fig. 4G–J).
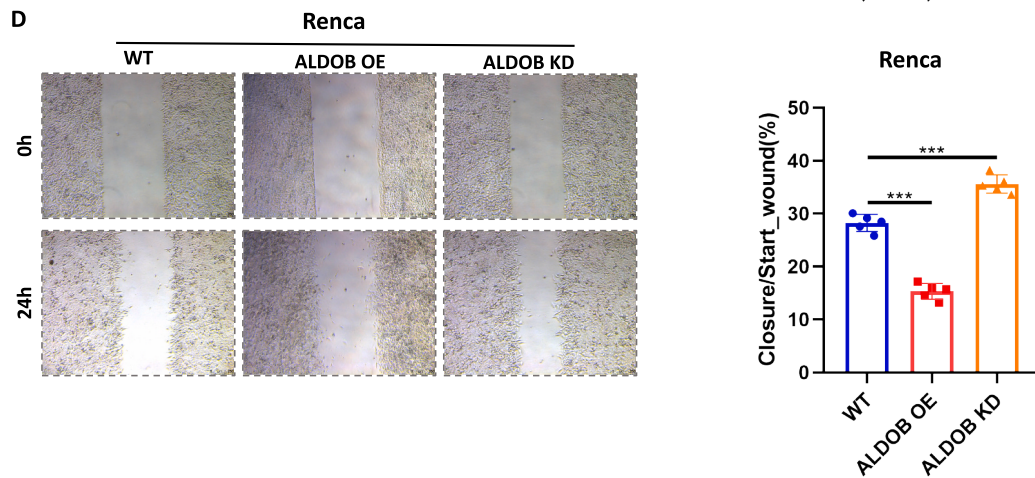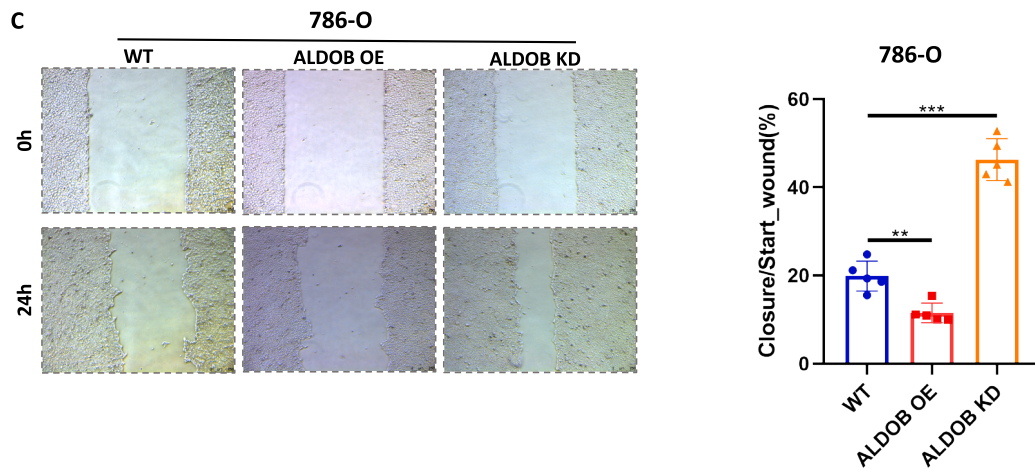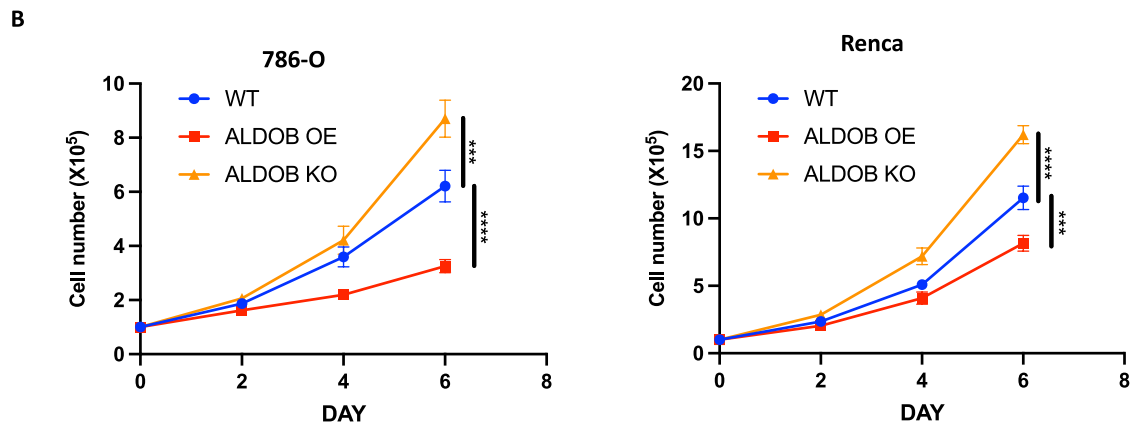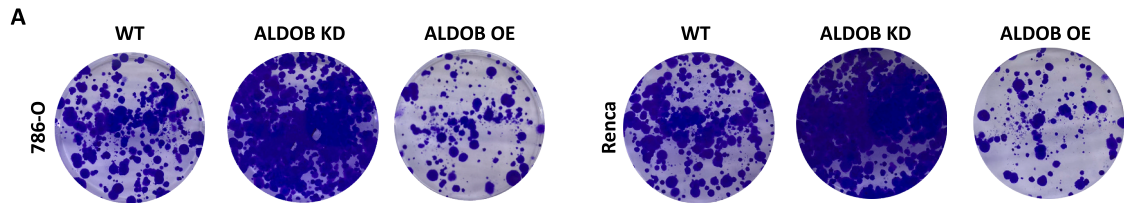
(caption on next page)

Fig. 3. ALDOB expression decreased growth and migration abilities of 786-O and Renca cells. Colony formation assays(A) and cell growth curves(B) were performed to assess the proliferation of ALDOB KD or ALDOB OE transduced 786-O and Renca cells.Cell wound healing assays in 786-O(C) and Renca(D) cells with or without ALDOB OE or KD. The width of cell wound healing was measured (n = 5/group). WT, wild type; ALDOB OE,ALDOB overexpression; ALDOB KD, ALDOB knockdown. Data were presented as means ± standard deviations. P values were determined by the one-way ANOVA, **P < 0.01, ***P < 0.001, ****P < 0.0001.

Strikingly, ALDOB knockdown significantly increased the growth rate of renal cancer tumors in mice, particularly in immune-intact Balb/c mice (Fig. 4H- I, Fig. 4K-L). Moreover, we observed a decrease in infiltrated CD8$^+$ T cells in the ALDOB KD Renca group (Supplementary Fig. 6B). Taken together, these in vivo experiments provide further validation that ALDOB plays a crucial role in tumor growth regulation. The differential effects of ALDOB overexpression and knockdown on tumor growth in immune-intact mice suggest its involvement in modulating anti-tumor immune responses, particularly through the regulation of CD8$^+$ T cell infiltration. These findings highlight the significance of ALDOB in the interplay between tumor growth and anti-tumor immunity in renal cancer.

4. Discussion

Kidney Renal Clear Cell Carcinoma (KIRC) is a prevalent and highly dangerous disease among kidney disorders. Therefore, the identification of effective biomarkers for early disease diagnosis is of utmost significance. Through the analysis of multiple public datasets (GSE100666, GSE79973, and GSE12606), we identified a total of 40 commonly deregulated genes, among which 12 were up-regulated and 24 were down-regulated. Using the standard of significant threshold of p < 0.01 in the Kaplan-Meier survival analysis results, we narrowed the range of prognostic biomarkers studied mainly to ALDOB, HEPACAM2, and DNAH11. Then, the ROC analysis results showed that ALDOB had better performance in the one-year, three-year and five-year periods. Ultimately, we focused on ALDOB for further research.

Aldolase B, a protein encoded by the ALDOB gene, demonstrates predominant expression in the adult liver, kidneys, and intestines [19]. Previous investigations have elucidated the crucial role of ALDOB in metabolism and glycolysis [20]. Primarily, ALDOB functions as a catalyst, facilitating the conversion of fructose 1-phosphate to dihydroxyacetone phosphate and glyceraldehyde [19]. Encouragingly, our pathway analysis aligns with these findings as we observe the enrichment of multiple upstream and downstream products and pathways related to glycolysis in the subgroup exhibiting high ALDOB expression. This discrepancy challenges our conventional understanding. Previous studies have convincingly demonstrated that cancer cells under aerobic conditions readily consume significant quantities of glucose via an "inefficient" form of glycolysis, also known as aerobic glycolysis or the Warburg effect, to satisfy their energy requirements for growth and proliferation [21,22]. However, in the case of KIRC, we observe lower ALDOB expression in tumors compared to adjacent tissues. While it would be premature to equate ALDOB expression solely with the occurrence of glycolysis, this intriguing observation highlights the need for further exploration. Moreover, we report a compelling correlation between the expression of ALDOB and the infiltration of diverse immune cell types, underscoring its potential as a predictive marker in the context of immunotherapy.

Furthermore, we discovered through additional studies that ALDOB serves as a significant prognostic marker in various cancer types [20,23–25]. Expanding upon these findings, we utilized the TIMER platform to analyze the expression patterns of ALDOB in numerous cancer types. Strikingly, in kidney-related cancers, the expression of ALDOB in tumor tissues exhibited a notable decrease compared to that in normal kidney tissues. Similarly, this trend was observed in breast cancer, intrahepatic cholangiocarcinoma, liver cancer, and other cancer types (Supplementary Fig. S1). These promising observations highlight the potential of ALDOB as a valuable asset in early cancer screening initiatives. Further investigation is warranted to fully explore its diagnostic and prognostic capabilities.

Despite the significant findings and potential implications of our research, it is important to acknowledge the limitations and gaps that remain in our study. Primarily, we recognize that we have not delved deeply enough into the underlying mechanisms by which ALDOB exerts its protective effect in KIRC. While we have established a correlation between ALDOB expression and various outcomes, we have yet to thoroughly investigate the specific molecular pathways and interactions through which this gene influences the development and progression of KIRC. Additionally, our analysis is primarily based on bioinformatics data and lacks direct experimental validation. Though bioinformatics approaches are valuable in generating hypotheses and identifying potential markers, further experimental validation is essential to confirm and expand upon our findings. Furthermore, our study focuses on the association between ALDOB expression and cancer-related outcomes without considering other confounding factors, such as patient characteristics and treatment regimens. Incorporating these factors would provide a more comprehensive understanding of ALDOB's role in cancer biology.

In conclusion, while our research sheds light on the potential significance of ALDOB expression as a prognostic marker and its association with immune cell infiltration in various cancers, more comprehensive and mechanistic investigations are needed to fully elucidate the underlying molecular mechanisms. Furthermore, experimental validation and consideration of confounding factors are essential for strengthening the clinical utility and broadening the scope of our findings.

Data availability statement

The datasets supporting the results and conclusions of this study were downloaded from the Cancer Genome Atlas (TCGA) (http://tcga-data.nci.nih.gov/tcga/) and Gene Expression Omnibus (GEO) (http://www.ncbi.nlm.nih.gov/geo/), and we thank TCGA and GEO for providing transcriptomics and clinicopathological data. The accession number are GSE100666, GSE5375, and GSE12606.
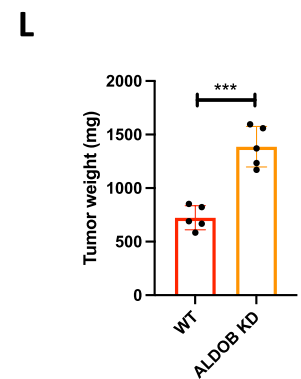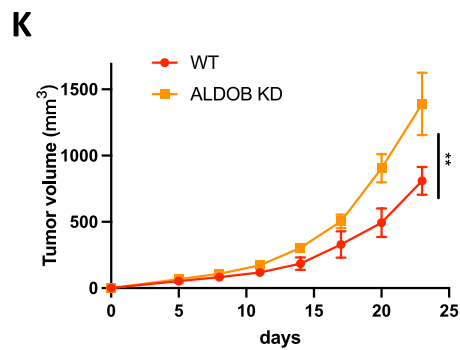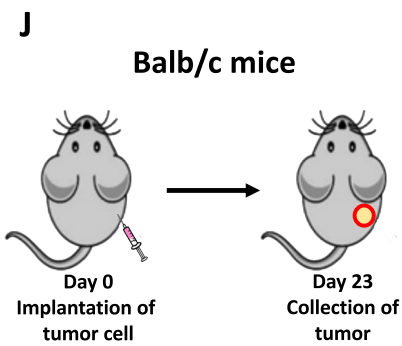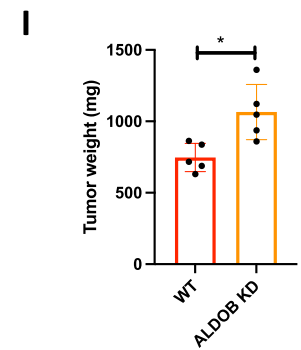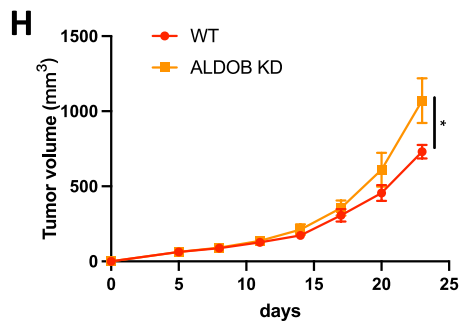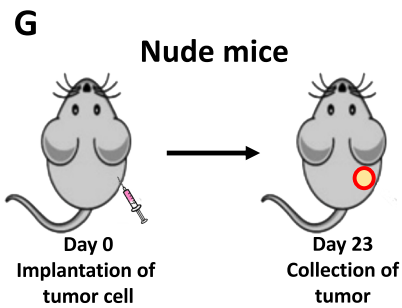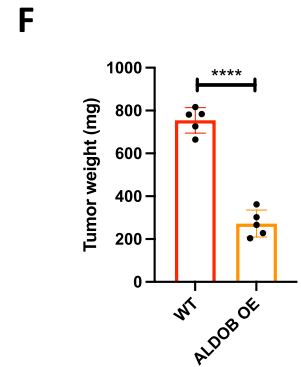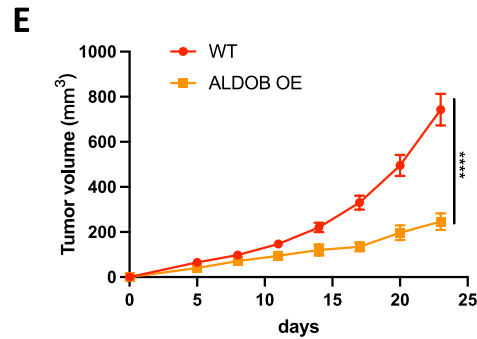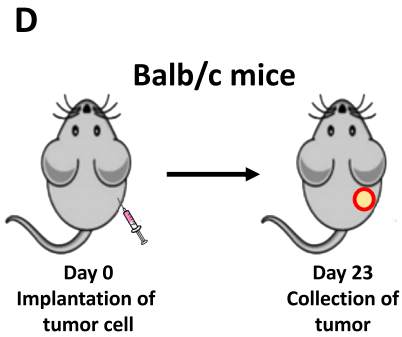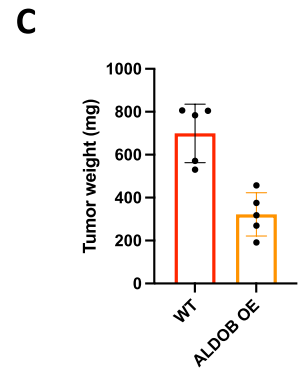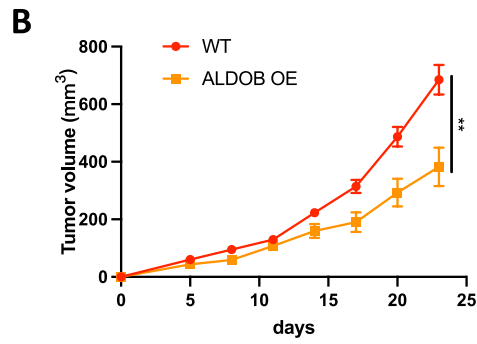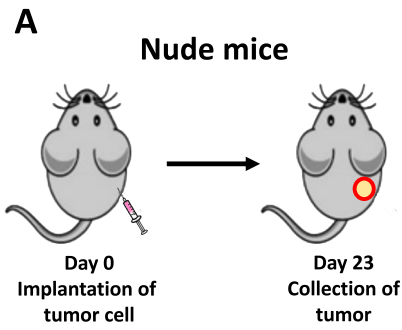
(caption on next page)

Fig. 4. ALDOB inhibits growth of Renca cell in vivo. WT nude mice (n = 5) were orthotopically inoculated with WT Renca cells and ALDOB OE Renca cells(A). Quantification of tumor growth (B) and tumor weight (C) of tumor. WT balb/c mice (n = 5) were orthotopically inoculated with WT Renca cells and ALDOB OE Renca cells(D). Quantification of tumor growth (E) and tumor weight (F) of tumor. WT nude mice (n = 5) were orthotopically inoculated with WT Renca cells and ALDOB KD Renca cells(G). Quantification of tumor growth (H) and tumor weight (I) of tumor. WT balb/c mice (n = 5) were orthotopically inoculated with WT Renca cells and ALDOB KD Renca cells(J). Quantification of tumor growth (K) and tumor weight (L) of tumor. P values were determined by the unpaired Student's t-test, *P < 0.05, **P < 0.01, ***P < 0.001, ****P < 0.0001.

Further inquiries can be directed to the corresponding authors.

Ethics statement

All animal experiments were approved by Research ethic committee of the Quzhou Affiliated Hospital of Wenzhou Medical University, Quzhou People's Hospital, ID of the approval: 20220121003.

CRediT authorship contribution statement

Xiao-yang Li: Writing – original draft. **You-yao Xu:** Writing – review & editing. **Sen-yan Wu:** Formal analysis. **Xi-xi Zeng:** Conceptualization. **Yan Zhou:** Formal analysis, Conceptualization. **Guo-bin Cheng:** Supervision.

Declaration of competing interest

The authors declare that they have no known competing financial interests or personal relationships that could have appeared to influence the work reported in this paper.

Appendix A. Supplementary data

Supplementary data to this article can be found online at https://doi.org/10.1016/j.heliyon.2024.e29368.

List of abbreviations

Abbreviation	Full name
KIRC	Kidney clear cell renal cell carcinoma
RCC	Renal cell carcinoma
DEGs	Different expression genes
FBS	Fetal bovine serum
GO	Gene Ontology
KEGG	Kyoto Encyclopedia of Genes and Genomes
IHC	Immunohistochemistry
ROC	receiver operating characteristic
TCGA	The Cancer Genome Atlas
GEO	Gene Expression Omnibus
IDH1/2	Isocitrate dehydrogenase 1/2
SPF	specific-pathogen-free

References

[1] R.L. Siegel, K.D. Miller, H.E. Fuchs, A. Jemal, Cancer Statistics, 2021, CA A Cancer J. Clin. 71 (2021) 7–33.
[2] B.C. Leibovich, et al., Histological subtype is an independent predictor of outcome for patients with renal cell carcinoma, J. Urol. 183 (2010) 1309–1315.
[3] J.J. Hsieh, et al., Renal cell carcinoma, Nat. Rev. Dis. Prim. 3 (2017) 17009.
[4] W.H. Chow, L.M. Dong, S.S. Devesa, Epidemiology and risk factors for kidney cancer, Nat. Rev. Urol. 7 (2010) 245–257.
[5] Z. Zhang, et al., Bioinformatics analysis reveals biomarkers with cancer stem cell characteristics in kidney renal clear cell carcinoma, Transl. Androl. Urol. 10 (2021) 3501–3514.
[6] J. Zhu, et al., Development and internal validation of nomograms for the prediction of postoperative survival of patients with grade 4 renal cell carcinoma (RCC), Transl. Androl. Urol. 9 (2020) 2629–2639.
[7] D. Xu, et al., The Evolving landscape of Noncanonical functions of metabolic enzymes in cancer and other pathologies, Cell Metabol. 33 (2021) 33–50.
[8] M. Notarnicola, et al., Fatty acid synthase hyperactivation in human colorectal cancer: relationship with tumor side and sex, Oncology 71 (2006) 327–332.
[9] M. Notarnicola, et al., Serum levels of fatty acid synthase in colorectal cancer patients are associated with tumor stage, J. Gastrointest. Cancer 43 (2012) 508–511.
[10] J. Mondesir, C. Willekens, M. Touat, S. de Botton, IDH1 and IDH2 mutations as novel therapeutic targets: current perspectives, J Blood Med 7 (2016) 171–180.
[11] H. Yang, D. Ye, K.L. Guan, Y. Xiong, IDH1 and IDH2 mutations in tumorigenesis: mechanistic insights and clinical perspectives, Clin. Cancer Res. 18 (2012) 5562–5571.
[12] Y. Liu, et al., The regulatory mechanisms and inhibitors of isocitrate dehydrogenase 1 in cancer, Acta Pharm. Sin. B 13 (2023) 1438–1466.
[13] B.J. Kim, J.H. Kim, H.S. Kim, D.Y. Zang, Prognostic and predictive value of VHL gene alteration in renal cell carcinoma: a meta-analysis and review, Oncotarget 8 (2017) 13979–13985.

[14] J. Coutinho, et al., Renal transplantation in Birt-Hogg-Dube syndrome: should we? BMC Nephrol. 19 (2018) 267.

[15] W. Wei, et al., Identification of key genes involved in the metastasis of clear cell renal cell carcinoma, Oncol. Lett. 17 (2019) 4321–4328.

[16] G.K. Smyth, Linear models and empirical bayes methods for assessing differential expression in microarray experiments, Stat. Appl. Genet. Mol. Biol. 3 (2004) Article3.

[17] T. Li, et al., TIMER: a Web server for comprehensive analysis of tumor-infiltrating immune cells, Cancer Res. 77 (2017) e108–e110.

[18] B. Chen, M.S. Khodadoust, C.L. Liu, A.M. Newman, A.A. Alizadeh, Profiling tumor infiltrating immune cells with CIBERSORT, Methods Mol. Biol. 1711 (2018) 243–259.

[19] Y.C. Chang, Y.C. Yang, C.P. Tien, C.J. Yang, M. Hsiao, Roles of aldolase family genes in human cancers and diseases, Trends Endocrinol. Metabol. 29 (2018) 549–559.

[20] N. Zhao, H. Xu, Pan-cancer analysis of aldolase B gene as a novel prognostic biomarker for human cancers, Medicine (Baltim.) 102 (2023) e33577.

[21] K. Garber, Energy deregulation: licensing tumors to grow, Science 312 (2006) 1158–1159.

[22] O. Warburg, On the origin of cancer cells, Science 123 (1956) 309–314.

[23] Y. Huang, et al., Identification and validation of a cigarette smoke-related five-gene signature as a prognostic biomarker in kidney renal clear cell carcinoma, Sci. Rep. 12 (2022) 2189.

[24] Y.F. Tian, et al., High expression of aldolase B confers a poor prognosis for rectal cancer patients receiving neoadjuvant chemoradiotherapy, J. Cancer 8 (2017) 1197–1204.

[25] Q. Li, et al., Aldolase B overexpression is associated with poor prognosis and promotes tumor progression by epithelial-mesenchymal transition in colorectal adenocarcinoma, Cell. Physiol. Biochem. 42 (2017) 397–406.